EPJ Web of Conferences **296**, 11005 (2024) https://doi.org/10.1051/epjconf/202429611005
Quark Matter 2023

New measurements of inclusive jet suppression and jet v_2 in Pb–Pb collisions at $\sqrt{s_{\rm NN}}$ = 5.02 TeV with ALICE

Nadine Alice Grünwald[1,*], on behalf of the ALICE Collaboration

[1]Physikalisches Institut Universität Heidelberg

Abstract. We report measurements of the inclusive charged-particle jet yield in central Pb–Pb collisions at $\sqrt{s_{\rm NN}}$ = 5.02 TeV. Uncorrelated background is suppressed by a novel mixed-event technique, enabling extension of the jet $R_{\rm AA}$ measurement down to $p_{\rm T}$ = 13.5 GeV/c, with kinematic overlap with RHIC jet measurements. We also present measurements of inclusive charged-particle jet v_2 in semi-central Pb–Pb collisions at $\sqrt{s_{\rm NN}}$ = 5.02 TeV, and azimuthal dependence of jet yield suppression for event topologies selected using event-shape engineering.

Collisions of heavy ions generate Quark-Gluon Plasma (QGP), a state of deconfined quarks and gluons (partons). Quarks and gluons from hard scatterings are generated prior to QGP formation, interacting with it ("jet quenching" [1]) before hadronizing into jets. Jet quenching has observable and calculable effects, including suppression of jet yield due to energy loss, modification of jet structure, and jet deflection. Jet-quenching measurements provide unique constraints on the structure and the dynamics of the QGP. In these proceedings we report ALICE measurements of several jet observables which probe the mechanisms underlying jet quenching in Pb–Pb collisions at $\sqrt{s_{\rm NN}}$ = 5.02 TeV.

Measurement of the inclusive charged-particle jet yield in central Pb–Pb collisions is challenging due to the large non-uniform uncorrelated background yield, the underlying event, especially for very low $p_{\rm T}$ jets. This analysis subtracts this background yield statistically using the novel mixed-event (ME) technique developed by the STAR collaboration [2]. This is the first application of the ME approach to inclusive jet measurements.

The data were recorded by ALICE during the 2018 Pb–Pb run at $\sqrt{s_{\rm NN}}$ = 5.02 TeV. Events in the 0–10% centrality interval are analysed. Charged-particle jets are reconstructed using the anti-$k_{\rm T}$ algorithm with a radius parameter of R = 0.3. The $p_{\rm T}$ of each reconstructed jet is corrected by an estimate of the mean underlying-event $p_{\rm T}$ density, i.e. $p_{\rm T,jet}^{\rm reco} = p_{\rm T,jet}^{\rm raw} - \rho A_{\rm jet}$, where ρ is the median background energy density and $A_{\rm jet}$ the jet area [3].

The ME population for the background-yield correction is constructed by mixing events separately in each of 9600 event subsets, categorized using multiplicity, position of collision vertex along beam axis, event plane angles Ψ_2 and Ψ_3, and the sum of track $p_{\rm T}$ in the event. Each ME contains no more than one track from a given event, so that the ME has no multi-hadron correlations. The full ME event population by construction reproduces the multiplicity, acceptance, and detector non-uniformity observed in real data. The same jet reconstruction procedure is carried out on the ME population as for the same-event (SE) population. The SE and ME populations are biased by a mild cut on the minimum $p_{\rm T}$ of the

*e-mail: gruenwald@physi.uni-heidelberg.de

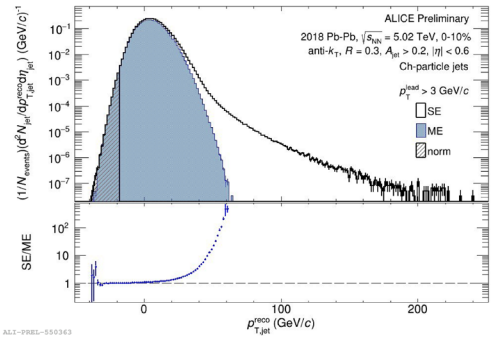

Figure 1. Raw SE (black) and ME (blue) jet $p_{\mathrm{T,jet}}^{\mathrm{reco}}$ distributions with $p_{\mathrm{T}}^{\mathrm{lead}} > 3$ GeV/c and $R = 0.3$. The range for the normalization of ME to SE is indicated by the shaded region. The ratio SE/ME is depicted in the lower panel.

leading track in the jet, in order to define a countable jet population corresponding to the product of a distinct hard-scattering process. The bias due to this cut is measured by varying the value of the cut.

Figure 1 shows the SE and ME jet $p_{\mathrm{T,jet}}^{\mathrm{reco}}$ distributions with leading track cut $p_{\mathrm{T}}^{\mathrm{lead}} > 3$ GeV/c. The yield ratio SE/ME (lower panel) is uniform over a wide range at negative $p_{\mathrm{T,jet}}^{\mathrm{reco}}$, showing that this region is dominated by combinatorial (background) jets [2, 4]. The ME distribution is normalized to the SE distribution within the shaded region.

The correlated (physical) jet yield is obtained by subtracting the normalized ME distribution from the SE distribution. After the subtraction the distribution must also be corrected for p_{T}-smearing due to background and instrumental effects, which is carried out using iterative Bayesian unfolding with a PYTHIA-generated particle-level distribution used as prior. The response matrix for the unfolding is obtained from PYTHIA jets embedded into the SE.

Figure 2, upper panel, shows the fully corrected charged-particle inclusive jet distributions in central Pb–Pb collisions for $p_{\mathrm{T}}^{\mathrm{lead}} > 3$ GeV/c and 4 GeV/c. The systematic uncertainty, depicted as a band, includes contributions from the ME procedure, the unfolding, the track DCA cut, and tracking efficiency. The lower panel shows the ratio of the distributions with $p_{\mathrm{T}}^{\mathrm{lead}} > 3$ GeV/c over $p_{\mathrm{T}}^{\mathrm{lead}} > 4$ GeV/c. The ratio is consistent with unity within 10% for $p_{\mathrm{T,jet}}^{\mathrm{ch}} > 13.5$ GeV/c, as indicated by the dashed line, corresponding, conservatively, to the region, in which the leading-track cut bias is negligible.

Figure 3 shows the charged-particle jet R_{AA} using these data with $p_{\mathrm{T}}^{\mathrm{lead}} > 3$ GeV/c, normalized by the unbiased charged-particle jet cross-section measured in pp collisions at $\sqrt{s_{\mathrm{NN}}} = 5.02$ TeV [5]. The quoted uncertainties represent the combined Pb–Pb and pp systematic and statistical uncertainties. The left panel compares this measurement to the charged-particle jet R_{AA} measured at RHIC. This is the first direct comparison of jet yield

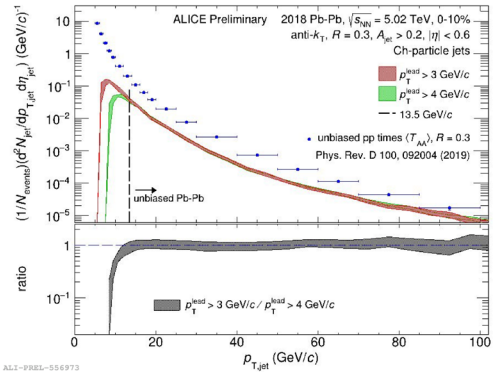

Figure 2. Corrected charged-particle jet distributions with leading track cuts of $p_{\mathrm{T}}^{\mathrm{lead}} > 3$ GeV/c (red) and $p_{\mathrm{T}}^{\mathrm{lead}} > 4$ GeV/c (green). The ratio between both distributions is shown in the lower panel. The published unbiased pp charged-particle jet distribution with the same jet radius is shown in blue [5].

suppression due to quenching at RHIC and the LHC, in the same kinematic range. The jet yield suppression at RHIC and the LHC is found to be compatible within the current uncertainties. However, we note that yield suppression arises from the combined effects of energy loss and spectrum shape. Because jet spectra are much steeper at RHIC than the LHC, the value of R_{AA} indicates smaller energy loss at RHIC than at the LHC, averaged over the reported jet population.

Figure 3, right panel, compares the measured R_{AA} distribution to model calculations incorporating jet quenching: the Monte Carlo codes JETSCAPE [6], MARTINI [7], and JEWEL recoils on and off [8], and an analytic calculation (Mehtar-Tani et al. [9]). In general all calculations describe the data well at higher p_{T}, but all models except JEWEL (recoils off) tend to disagree with the data at low p_{T}. This is the first comparison of these models at such low p_{T} at the LHC, where wake effects are predicted to be significant [10].

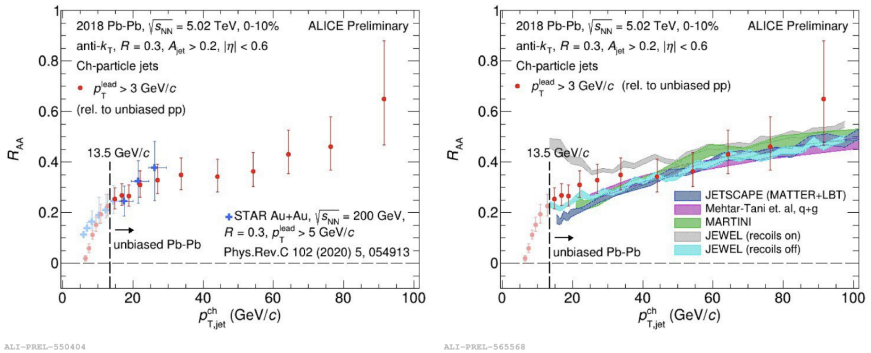

Figure 3. Charged-particle jet R_{AA} (red) calculated relative to the unbiased pp charged-particle jet distribution [5]. Above the dashed line at $p_{\mathrm{T,jet}}^{\mathrm{ch}} > 13.5$ GeV/c the Pb–Pb charged-particle jet distribution is unbiased. Left: Comparison to the STAR R_{AA} (blue) [11]. Right: Comparison to different model calculations. See text for details.

To get access to the mechanisms of jet energy loss, the pathlength dependence can be measured using the event plane orientation. The difference in the in-plane and out-of-plane jet yield is parameterized by the inclusive charged-particle jet v_2. Figure 4 shows the charged-particle jet v_2 measured in semi-central (30–50%) Pb–Pb collisions at $\sqrt{s_{\mathrm{NN}}} = 5.02$ TeV. The charged-particle jet reconstruction is done with the anti-k_{T} algorithm and $R = 0.2$. In addition, a leading track cut $p_{\mathrm{T}}^{\mathrm{lead}} > 5$ GeV/c is applied. The systematic uncertainties are dominated by the uncertainty from the determination of the event-plane and the prior functions in the unfolding. The measured positive charged-particle jet v_2 is a result of the larger suppression of the out-of-plane jets due to a larger average pathlength. The suppression is larger at low p_{T} because of a steeper spectrum at low p_{T}, which results in a larger suppression and thus a larger v_2 and a smaller R_{AA} as shown above. The measured v_2 is consistent with the previous ALICE charged-particle jet v_2 measurement at $\sqrt{s_{\mathrm{NN}}} = 2.76$ TeV [12] and the ATLAS results in the overlapping p_{T} bins [13].

A more differential measurement of the pathlength dependence of jet energy loss can be performed by using event-shape engineering (ESE) to select a specific event topology [14]. With ESE the events are classified according to their anisotropy in a centrality class. For the classification, the reduced flow vector q_2 is calculated. For large/small q_2 values a more elliptical/isotropic event shape is expected. In the analysis, the events are separated into q_2-large and q_2-small event samples, which contain 30% of events with the largest and

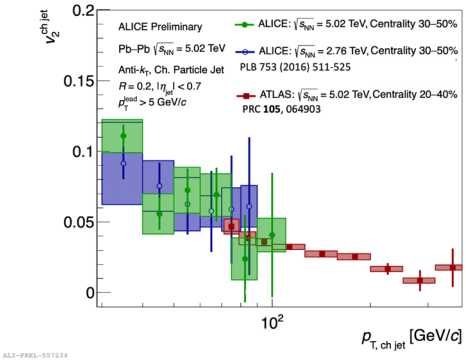

Figure 4. Charged-particle jet v_2 as a function of $p_{\mathrm{T,jet}}^{\mathrm{ch}}$ measured at $\sqrt{s_{\mathrm{NN}}}$ = 5.02 TeV and 30–50% centrality (green). The published ALICE v_2 results measured at $\sqrt{s_{\mathrm{NN}}}$ = 2.76 TeV with the same centrality range are shown in blue [12] and ATLAS results measured at $\sqrt{s_{\mathrm{NN}}}$ = 5.02 TeV with 20–40% centrality are shown in red [13].

smallest q_2. The jet reconstruction is performed with the anti-k_{T} algorithm, $R = 0.2$ and 0.4 with a leading track cut of $p_{\mathrm{T}}^{\mathrm{lead}} > 5$ GeV/c. A jet wise background subtraction, unfolding, and efficiency corrections are done. Jets are considered in- and out-of-plane when they are reconstructed within ±30 degrees in azimuth of the in- and out-of-plane axis, respectively. More details are described in Ref. [14].

The ratios of the charged-particle jet yields are shown for the q_2-large and q_2-small event samples separately in Fig. 4 of Ref. [14]. While in the azimuthally averaged measurement only a small difference between the jet yields in the q_2-large and q_2-small event samples was observed, a larger effect is observed in the azimuthally differential measurement. A clear suppression of the out-of-plane jets compared to the in-plane jets is measured. This suppression could be further enhanced at $p_{\mathrm{T,jet}}^{\mathrm{ch}} < 50$ GeV/c for the smaller jet radius of $R = 0.2$ when only the q_2-large events are considered. This measurement shows that under the application of ESE, the relative difference between in- and out-of-plane jet pathlengths can be increased, which is consistent with the expectation from Trajectum calculations [15].

References

[1] R. Baier, Y.L. Dokshitzer, A.H. Mueller, S. Peigne, D. Schiff, Nucl. Phys. B **484**, 265 (1997), hep-ph/9608322
[2] L. Adamczyk et al. (STAR), Phys. Rev. C **96**, 024905 (2017), 1702.01108
[3] M. Cacciari, G.P. Salam, G. Soyez, Eur. Phys. J. C **72**, 1896 (2012), 1111.6097
[4] J. Adam et al. (ALICE), JHEP **09**, 170 (2015), 1506.03984
[5] S. Acharya et al. (ALICE), Phys. Rev. D **100**, 092004 (2019), 1905.02536
[6] J.H. Putschke et al. (2019), 1903.07706
[7] S. Shi, R. Modarresi Yazdi, C. Gale, S. Jeon, Phys. Rev. C **107**, 034908 (2023), 2212.05944
[8] R. Kunnawalkam Elayavalli, K.C. Zapp, JHEP **07**, 141 (2017), 1707.01539
[9] Y. Mehtar-Tani, D. Pablos, K. Tywoniuk, Phys. Rev. Lett. **127**, 252301 (2021), 2101.01742
[10] S. Acharya et al. (ALICE) (2023), 2308.16131
[11] J. Adam et al. (STAR), Phys. Rev. C **102**, 054913 (2020), 2006.00582
[12] J. Adam et al. (ALICE), Phys. Lett. B **753**, 511 (2016), 1509.07334
[13] G. Aad et al. (ATLAS), Phys. Rev. C **105**, 064903 (2022), 2111.06606
[14] S. Acharya et al. (ALICE) (2023), 2307.14097
[15] C. Beattie, G. Nijs, M. Sas, W. van der Schee, Phys. Lett. B **836**, 137596 (2023), 2203.13265